Supporting Information

Ultrathin Single-Crystalline Vanadium Pentoxide Nanoribbons Constructed 3D Networks for Superior Energy Storage

Liujun Cao,[a,b] Jixin Zhu,[c] Yanhong Li,[d] Peng Xiao,[d] Yunhuai Zhang,[a] Shengtao Zhang*[a], Shubin Yang*[b,e]

[a]School of Chemistry and Chemical Engineering, Chongqing University, Chongqing, 400044, China. Email: stzhang@cqu.edu.cn
[b]Department of Mechanical Engineering & Materials Science, Rice University, Houston, Texas 77005, USA
[c]TUM CREATE, 1 CREATE Way, #10-02 CREATE Tower, 138602, Singapore
[d]School of Physics, Chongqing University, Chongqing, 400044, China
[e]School of Materials Science and Engineering, Beihang University,
Beijing, 100191, China. Email: yangshubin@buaa.educn

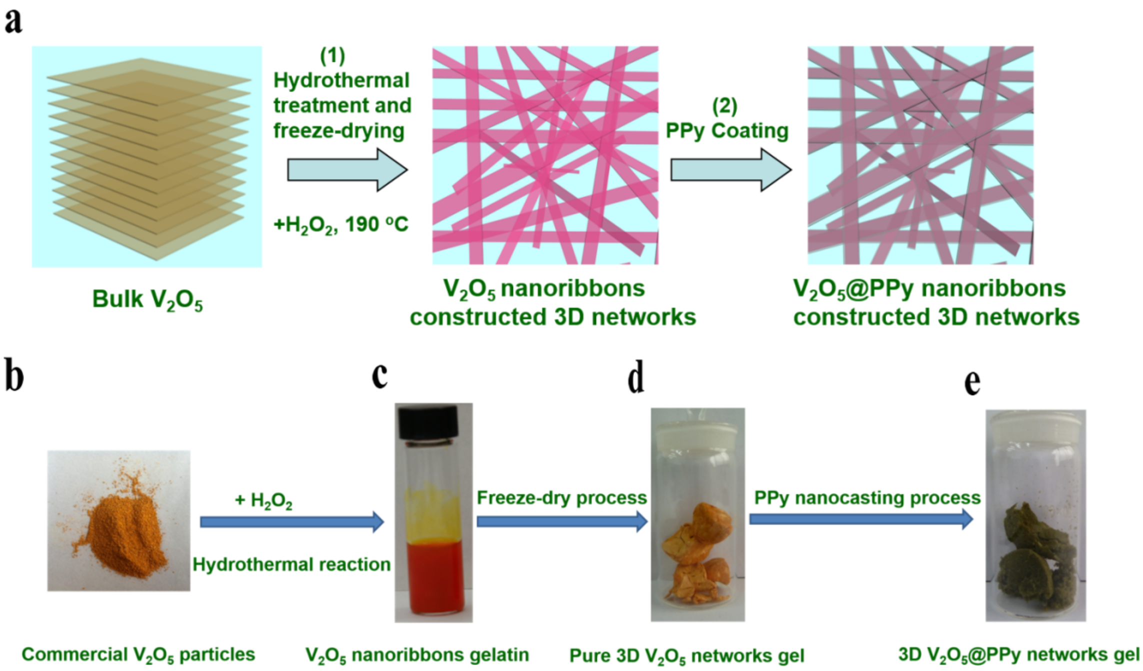

Figure S1. (a) Schematic illustration for the fabrication of 3D V_2O_5@PPy networks by a combined hydrothermal synthesis, freeze-drying and subsequent PPy coating. The optical photos of (b) commercial V_2O_5 particles, (c) as-prepared V_2O_5 nanoribbon gelatin, (d) pure 3D V_2O_5 network gel produced by freeze-drying process, and (e) 3D V_2O_5@PPy network produced by PPy nanocasting process.

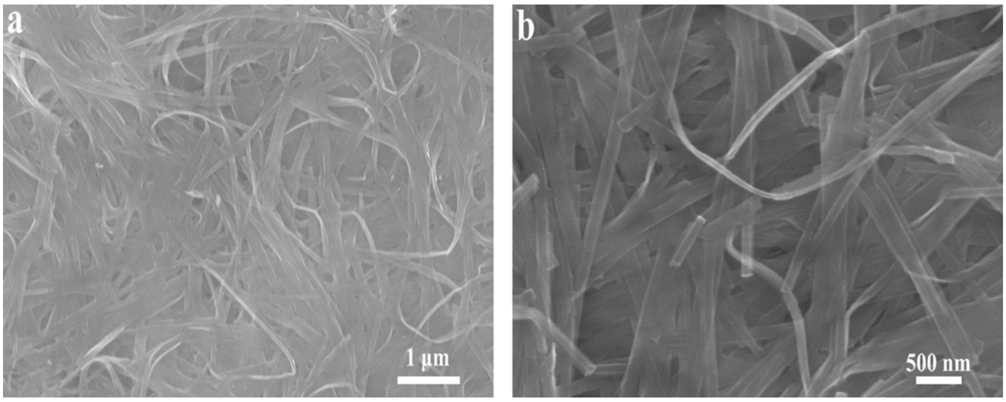

Figure S2. (a) and (b) SEM images with different magnifications for V_2O_5 sample obtained by normal drying method, demonstrating that the V_2O_5 nanoribbons are strongly aggregated and compactly stacked together without using freeze-drying process.

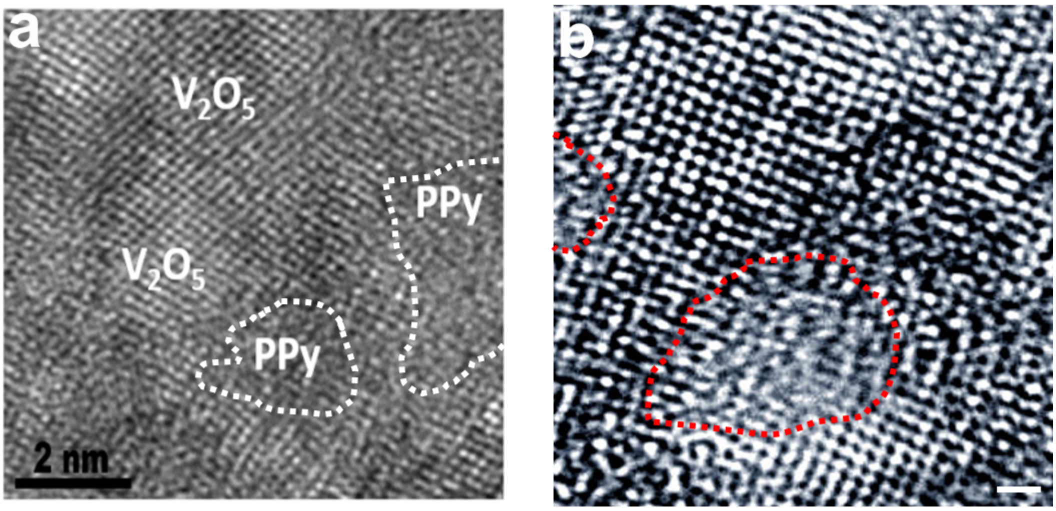

Figure S3. (a) and (b) HRTEM images of V_2O_5@PPy ribbon with different magnifications. (a) HRTEM image shows the incontinuous structure of PPy on the surface of V_2O_5 well-crystalline ribbon (marked by white dot line). (b) HRTEM image discloses the interfaces between PPy nanograins and well-defined V_2O_5 (marked by red dot line) (scale bar, 2 nm).

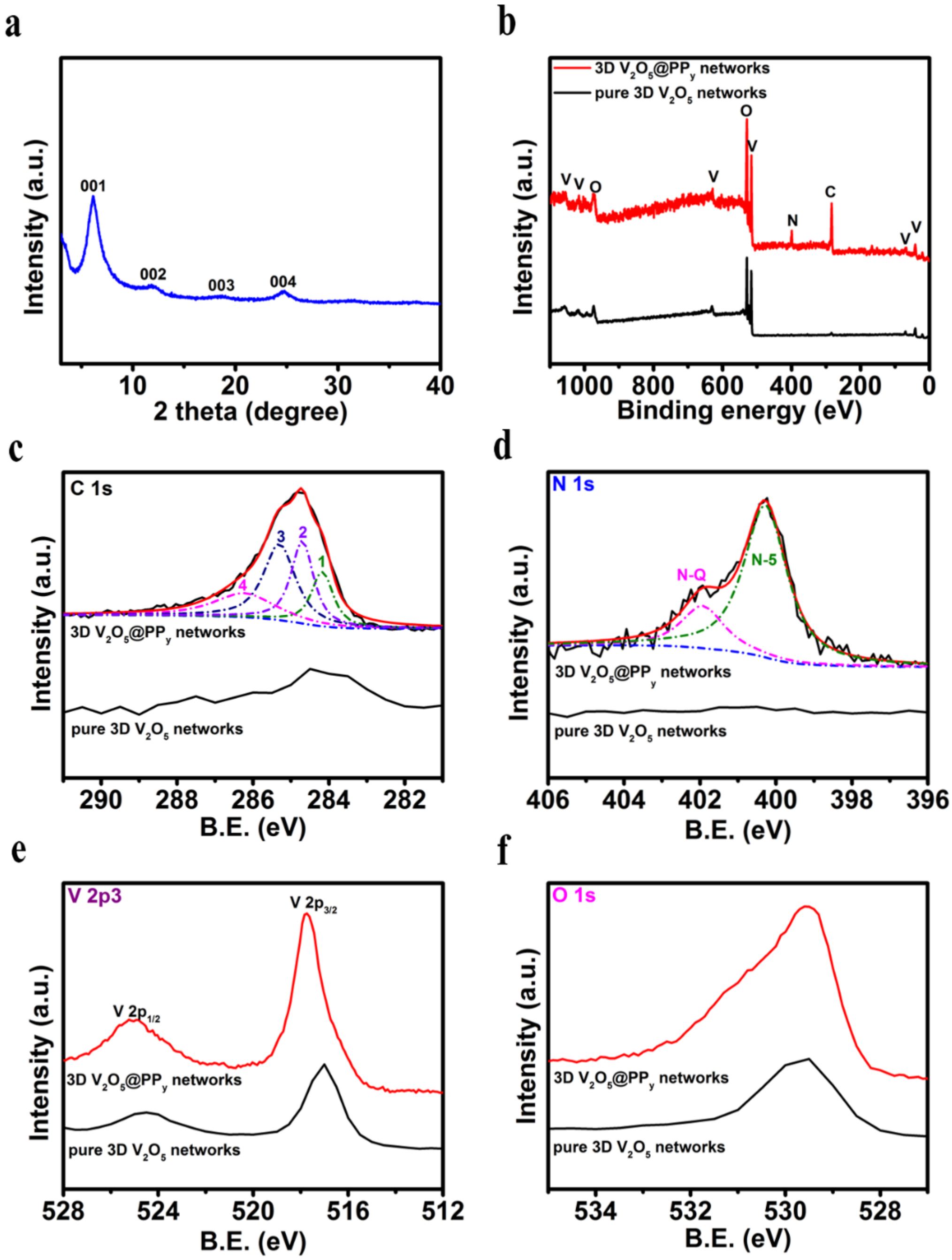

Figure S4. (a) XRD patterns of 3D V_2O_5@PPy network, showing a main peak at 6.1°, and three small peaks at 12.2°, 18.3° and 24.4°, well consistent with those of pure 3D V_2O_5 network. (b) XPS surveys of 3D V_2O_5@PPy network and pure 3D V_2O_5 network. High resolution spectra of (c) C1s, (d) N1s, (e) V2p3 and (f) O1s, respectively.

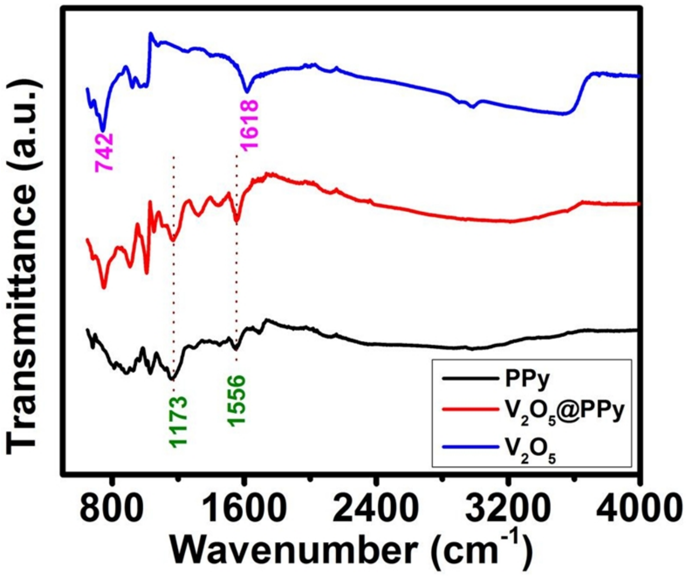

Figure S5. The Fourier transform infrared spectroscopy (FTIR) spectra of PP_y, 3D V_2O_5 network and V_2O_5@PP_y network. There is a band at 1556 cm^{-1}, attributed to the fundamental vibration of pyrrole ring, and another band at 1173 cm^{-1} is characteristic of the C-N stretching vibration, demonstrating the presence of PP_y in our 3D V_2O_5@PP_y network.

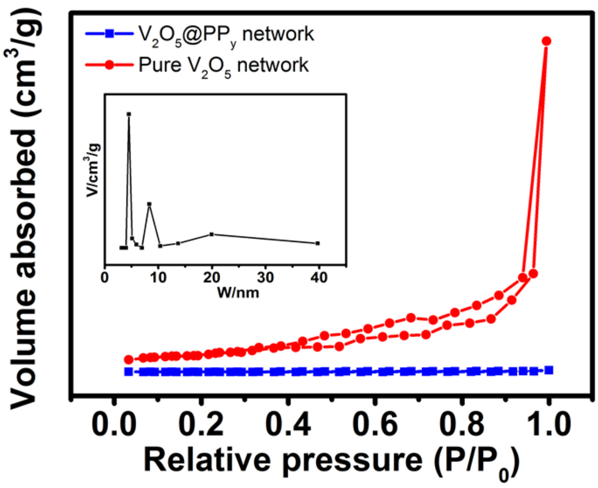

Figure S6. Nitrogen adsorption/desorption isothermal of the 3D pure V_2O_5 network and V_2O_5@PP_y network, showing the surface area of 130 and 35 m^2g^{-1}, respectively. Insert was the pore size distribution of 3D pure V_2O_5 network.

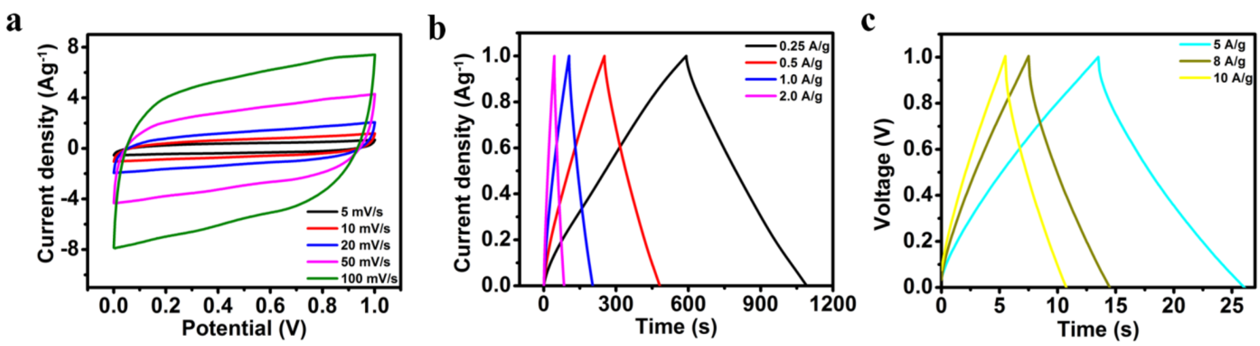

Figure S7. The electrochemical performances of a symmetric supercapacitor using 3D V_2O_5@PP_y network as electrode material. (a) CV curves at various scan rates from 5 to 100 mV s^{-1}, (b-c) Galvanostatic charge-discharge curves at different current densities from 0.25 to 10 A g^{-1}.

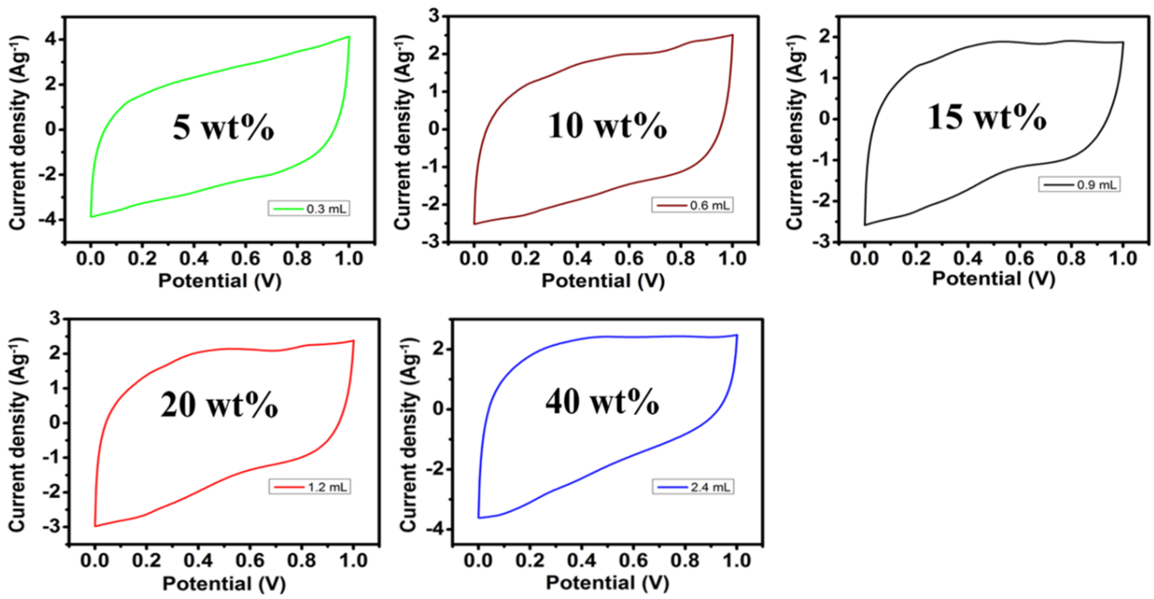

Figure S8. The influence of of PP_y content on the cyclic voltammetry (CV) curves of 3D V_2O_5@PP_y networks. The shape of the CV curve become distinctly distorted with increasing PP_y content from 5 wt% to 40 wt% at the scan rate of 20 mV s^{-1} in 1.0 M Na_2SO_4 aqueous solution.

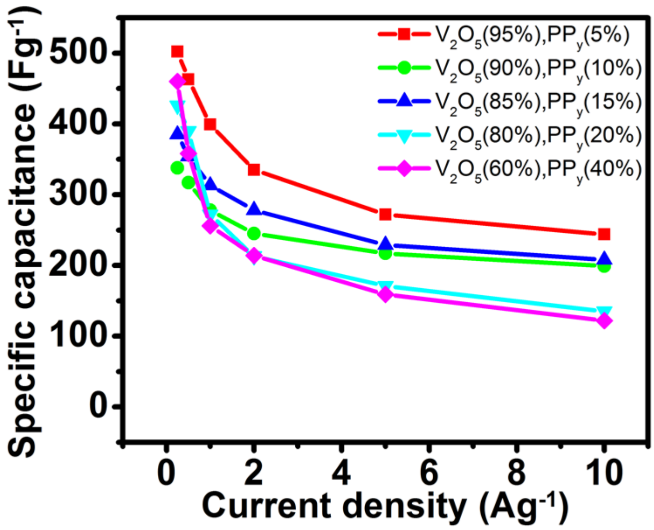

Figure S9. The influence of PP_y content on rate capabilities of 3D V_2O_5@PP_y networks at different current densities. The specific capacitances calculated from charge-discharge curves largely decreases with increasing PP_y coating amount (from 5 wt% to 40 wt%).

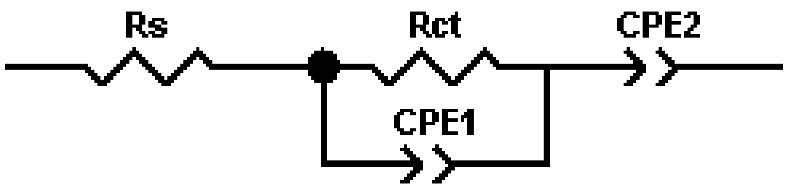

Figure S10. The equivalent circuit diagram used for fitting the EIS profiles of 3D V_2O_5@PP_y network, pure 3D V_2O_5 network and V_2O_5 particles@PP_y.

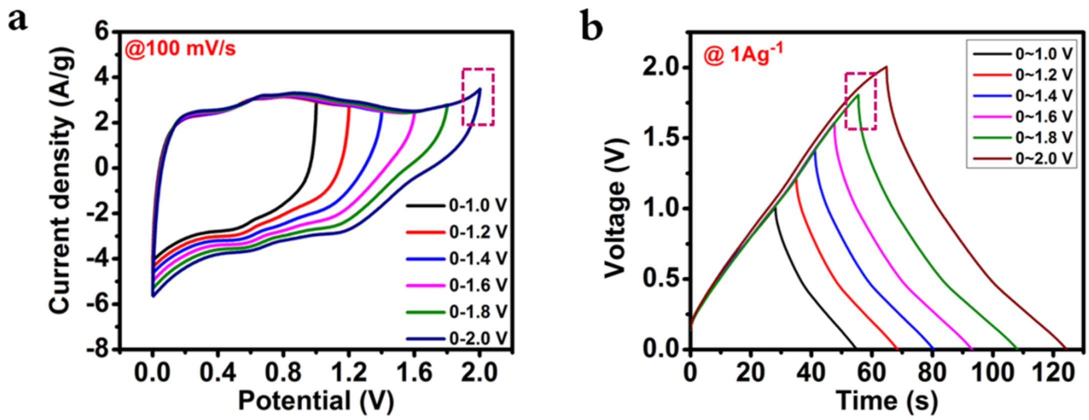

Figure S11. (a) A series of CV measurements at 100 mV s^{-1}, while the operating potential is extended to 2.0 V, a distinct peak appears at the end of CV (select area in (a)), ascribed to the evolution of oxygen. (b) Galvanostatic charge/discharge plots at 1A g^{-1} with the potential window between 1.0 and 2.0 V, when the voltage reach 2.0 V, the charge-discharge curve is no longer symmetric (select area in (b)) indicating non-capacitive behavior.

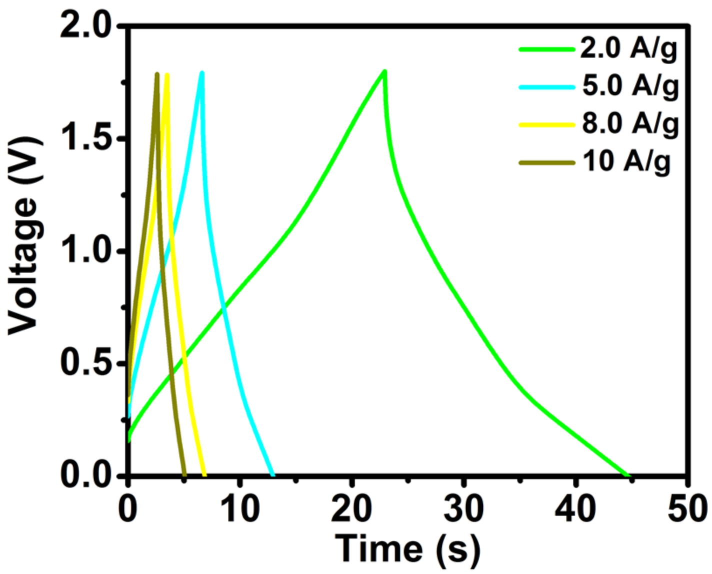

Figure S12. Galvanostatic charge/discharge plots of 3D V_2O_5@PPy network// 3D rGO asymmetric supercapacitor at high current densities between 2 and 10 A g^{-1} under the potential window of 1.8 V.

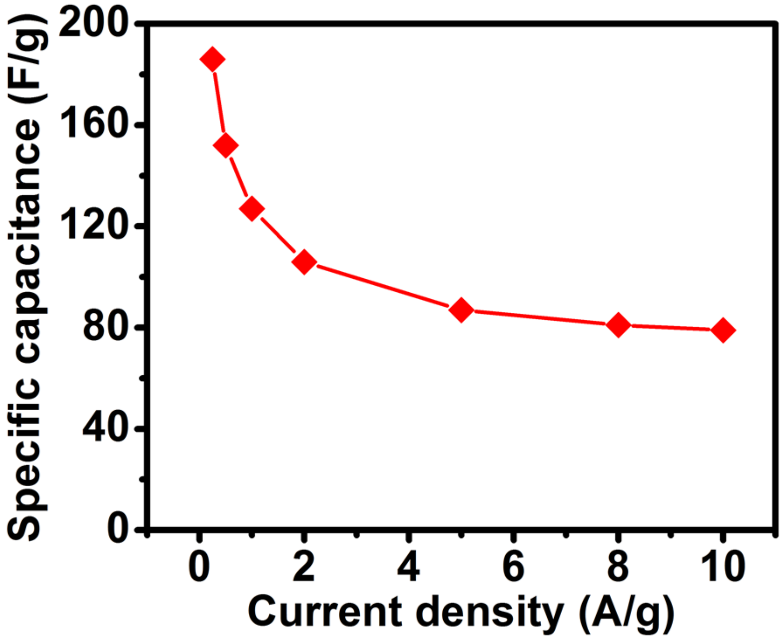

Figure S13. Specific capacitance of V_2O_5@PP_y network// 3D rGO asymmetric supercapacitorl under different current densities (from 0.25 to 10 A g^{-1}) calculated from galvanostatic charge/discharge plots.

Table 1. The kinetics parameters of 3D V_2O_5@PP_y network, pure 3D V_2O_5 network and V_2O_5 particles@PPy.

Electrodes	R_s (Ω)	R_{ct} (Ω)
3D V_2O_5@PP_y network	0.6	5.1
Pure 3D V_2O_5 network	0.7	7.4
V_2O_5@PP_y particles	1.0	8.6